

# Chapter 2

## Crane Mathematic Model

**Abstract** This chapter examines the dynamics of overhead cranes. Concerning single-pendulum-type overhead cranes, their equations of motion are first presented by means of its Euler–Lagrange equations. Subsequently, the equations of motion are extended to double-pendulum-type overhead cranes. The two models are presented as references for examples throughout this book. Since the two models are established under some ideal assumptions, some uncertainties associated with real applications are discussed next. In addition, the chapter proceeds with the analysis of oscillations for pendulum-type motions on the basis of linearized models of the two types of overhead cranes. The analysis distills the essential properties of each.

**Keywords** Overhead crane modeling · Single-pendulum dynamics · Double-pendulum dynamics · Uncertainty

### 2.1 Modeling of Single-Pendulum-Type Cranes

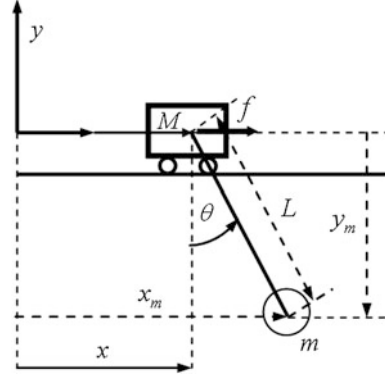
#### 2.1.1 Modeling

Figure 2.1 shows the coordinate system of an overhead crane system with its payload. Apparently, the crane system consists of two subsystems, i.e., trolley and payload [1]. The former is driven by a force. The latter is suspended from the trolley by a rope.

Other symbols in Fig. 2.1 are described as the trolley mass  $M$ , the payload mass  $m$ , the rope length  $L$ , the swing angle of the payload with respect to the vertical line  $\theta$ , the trolley position with respect to the origin  $x$ , and the driven force applied to the trolley  $f$ .

Consider that the crane in Fig. 2.1 is static and the payload is in its downward position. If the trolley moves toward the right direction by a positive driven force, then the payload will rotate clockwise. Apparently, the payload angle  $\theta$  is inherently

**Fig. 2.1** Structure of the single-pendulum-type overhead crane system



a pendulum-type motion. For the purpose of simplification, the following assumptions [2] are given.

- The payload is regarded as a material particle.
- The rope is considered as an inflexible rod.
- Compared with the payload mass, the rope mass is ignored.
- The trolley moves in the  $x$ -direction.
- The payload moves on the  $x$ - $y$  surface.
- No friction exists in the system.

Using Lagrangian method, the Lagrangian equation with respect to the generalized coordinate  $q_i$  [3] can be obtained as

$$\frac{d}{dt} \left( \frac{\partial La}{\partial \dot{q}_i} \right) - \frac{\partial La}{\partial q_i} = T_i, \quad (2.1)$$

where  $i = 1, 2$ ,  $La = K - P$  ( $K$  means the system kinetic energy and  $P$  denotes the system potential energy.),  $q_i$  is the generalized coordination (here,  $q_1$  and  $q_2$  indicate  $x$  and  $\theta$ , respectively), and  $T_i$  is the external force.

According to the assumption that the payload is regarded as a material particle, the system kinetic energy in Fig. 2.1 can be depicted as

$$K = \frac{1}{2} M \dot{x}^2 + \frac{1}{2} m v^2 \quad (2.2)$$

here,  $v$  is a vector and it denotes the payload velocity, defined as

$$v^2 = v_x^2 + v_y^2, \quad (2.3)$$

where  $v_x = \dot{x} + L\dot{\theta} \cos \theta$  and  $v_y = -L\dot{\theta} \sin \theta$ . Note that the payload is assumed to be a particle such that its moment of inertia is not considered in (2.2). When it is failed

to assume that the payload is a particle, its moment of inertia has to be taken into considerations.

From Fig. 2.1, the potential energy of the trolley subsystem is kept unchanged. Owing to this fact, the system potential energy in Fig. 2.1 is only exhibited by the potential energy of the payload subsystem, defined as

$$P = mgL(1 - \cos \theta) \quad (2.4)$$

Here,  $g$  is the gravitational acceleration. From (2.2) and (2.4),  $La$  has the form

$$La = K - P = \frac{1}{2}M\dot{x}^2 + \frac{1}{2}m\dot{v}^2 - mgL(1 - \cos \theta) \quad (2.5)$$

Consider the variable  $x$ . Differentiating  $La$  with respect to  $x$  in (2.5) yields

$$\frac{\partial La}{\partial x} = 0 \quad (2.6)$$

Differentiating  $La$  with respect to  $\dot{x}$  in (2.5) yields

$$\frac{\partial La}{\partial \dot{x}} = M\dot{x} + m(\dot{x} + L\dot{\theta} \cos \theta) \quad (2.7)$$

Further, differentiating (2.7) with respect to time  $t$  can have

$$\frac{d}{dt} \left( \frac{\partial La}{\partial \dot{x}} \right) = M\ddot{x} + m(\ddot{x} + L\ddot{\theta} \cos \theta - L\dot{\theta}^2 \sin \theta) \quad (2.8)$$

Finally, the Lagrangian equation with respect to  $x$  has the form

$$\frac{d}{dt} \left( \frac{\partial La}{\partial \dot{x}} \right) - \frac{\partial La}{\partial x} = (m + M)\ddot{x} + mL(\ddot{\theta} \cos \theta - \dot{\theta}^2 \sin \theta) = f \quad (2.9)$$

Consider the variable  $\theta$ . Differentiating  $La$  with respect to  $\theta$  in (2.5) yields

$$\begin{aligned} \frac{\partial La}{\partial \theta} &= m[(\dot{x} + L\dot{\theta} \cos \theta)(-L\dot{\theta} \sin \theta) \\ &\quad + (L\dot{\theta} \sin \theta)(L\dot{\theta} \cos \theta)] - mgL \sin \theta \\ &= -mL\dot{x} \sin \theta - mgL \sin \theta \end{aligned} \quad (2.10)$$

Differentiating  $La$  with respect to  $\dot{\theta}$  in (2.5) yields

$$\begin{aligned} \frac{\partial La}{\partial \dot{\theta}} &= m[(\dot{x} + L\dot{\theta} \cos \theta)(L \cos \theta) + (-L\dot{\theta} \sin \theta)(-L\dot{\theta} \sin \theta)] \\ &= mL\dot{x} \cos \theta + mL^2\dot{\theta} \end{aligned} \quad (2.11)$$

Further, differentiating (2.11) with respect to time  $t$  can have

$$\frac{d}{dt} \left( \frac{\partial La}{\partial \dot{\theta}} \right) = mL\ddot{x} \cos \theta - mL\dot{x}\dot{\theta} \sin \theta + mL^2\ddot{\theta} \quad (2.12)$$

Finally, the Lagrangian equation with respect to  $\theta$  has the form

$$\frac{d}{dt} \left( \frac{\partial La}{\partial \dot{\theta}} \right) - \frac{\partial La}{\partial \theta} = mL\ddot{x} \cos \theta + mL^2\ddot{\theta} + mgL \sin \theta = 0 \quad (2.13)$$

From (2.9) and (2.13), the dynamic model [4] of this overhead crane system with respect to  $x$  and  $\theta$  can be obtained by means of the Lagrangian method.

$$(m + M)\ddot{x} + mL(\ddot{\theta} \cos \theta - \dot{\theta}^2 \sin \theta) = f \quad (2.14)$$

$$\ddot{x} \cos \theta + L\ddot{\theta} + g \sin \theta = 0 \quad (2.15)$$

Further, the above dynamic model composed of (2.14) and (2.15) can be transformed to the following state space model [5], formulated as

$$\begin{aligned} \dot{x}_1 &= x_2 \\ \dot{x}_2 &= f_1(\mathbf{x}) + b_1(\mathbf{x})u \\ \dot{x}_3 &= x_4 \\ \dot{x}_4 &= f_2(\mathbf{x}) + b_2(\mathbf{x})u \end{aligned} \quad (2.16)$$

Here,  $\mathbf{x} = [x_1, x_2, x_3, x_4]^T$ ;  $x_1 = x$ ;  $x_3 = \theta$ ;  $x_2$  is the trolley velocity;  $x_4$  is the angular velocity of the load;  $u$  is the control input; and  $f_i$  and  $b_i$  ( $i = 1, 2$ ) are described as

$$\begin{aligned} f_1(\mathbf{x}) &= \frac{MLx_4^2 \sin x_3 + mg \sin x_3 \cos x_3}{M + m \sin^2 x_3} \\ b_1(\mathbf{x}) &= \frac{1}{M + m \sin^2 x_3} \\ f_2(\mathbf{x}) &= \frac{(M + m)g \sin x_3 + mLx_4^2 \sin x_3 \cos x_3}{(M + m \sin^2 x_3)L} \\ b_2(\mathbf{x}) &= \frac{\cos x_3}{(M + m \sin^2 x_3)L} \end{aligned}$$

Equation (2.16) formulates the state space model of this single-pendulum-type overhead crane system. In (2.16), four state variables can depict this dynamic system. As far as state-variable-based control methods are concerned, the four states can be employed and a diversity of control approached can be achieved.

Note that the model (2.16) is ideal and it contains no uncertainties. Due to imperfect modeling and effects of environment, it is impossible to avoid uncertainties and external disturbance in real dynamical systems. In reality, overhead crane systems often are operated under uncertainty conditions such as parameter variations, unmodeled dynamics, skidding and slipping, etc. Considering the possible effects of these uncertainties, the dynamic model of the overhead crane in Fig. 2.1 can have the form

$$\begin{aligned}\dot{x}_1 &= x_2 \\ \dot{x}_2 &= f_{10}(\mathbf{x}) + b_{10}(\mathbf{x})u \\ \dot{x}_3 &= x_4 \\ \dot{x}_4 &= f_{20}(\mathbf{x}) + b_{20}(\mathbf{x})u\end{aligned}\tag{2.17}$$

In (2.17)  $f_{i0}(\mathbf{x}) = f_i(\mathbf{x}) + \Delta f_i(\mathbf{x})$ ,  $b_{i0}(\mathbf{x}) = b_i(\mathbf{x}) + \Delta b_i(\mathbf{x})$  ( $i = 1, 2$ ), where  $f_i(\mathbf{x})$  and  $b_i(\mathbf{x})$  are the nominal parts of  $f_{i0}(\mathbf{x})$  and  $b_{i0}(\mathbf{x})$ , respectively. Both  $f_i(\mathbf{x})$  and  $b_i(\mathbf{x})$  are formulated in (2.16). Without loss of generality, the terms depicting modeling errors and parameter variations,  $\Delta f_{i0}(\mathbf{x})$  and  $\Delta b_{i0}(\mathbf{x})$  are assumed to be differentiable with respect to time  $t$ .

### 2.1.2 Model with Uncertainties

Uncertainties can be categorized as matched uncertainties and unmatched uncertainties [6]. The uncertainties are matched if and only if the uncertainties enter a dynamical system from the control tunnel. In (2.17), the so-called matched uncertainties mean

$$\Delta f_{i0}(\mathbf{x}) \text{ and } \Delta b_{i0}(\mathbf{x}) \in \text{span}\{b_i(\mathbf{x})\}\tag{2.18}$$

Explicitly, (2.18) can be written as

$$\begin{aligned}\Delta f_{i0}(\mathbf{x}) &= b_i(\mathbf{x})\Delta\tilde{f}_i(\mathbf{x}) \\ \Delta b_{i0}(\mathbf{x}) &= b_i(\mathbf{x})\Delta\tilde{b}_i(\mathbf{x})\end{aligned}$$

Substituting (2.18) into (2.17) yields

$$\begin{aligned}\dot{x}_2 &= f_1(\mathbf{x}) + b_1(\mathbf{x})[u + \Delta\tilde{b}_1(\mathbf{x})u + \Delta\tilde{f}_1(\mathbf{x})] \\ \dot{x}_4 &= f_2(\mathbf{x}) + b_2(\mathbf{x})[u + \Delta\tilde{b}_2(\mathbf{x})u + \Delta\tilde{f}_2(\mathbf{x})]\end{aligned}\tag{2.19}$$

Apparently, all the uncertainties in (2.19) enter the dynamic model (2.17) by the control tunnel, indicating that they are matched. Such an entering tunnel makes this kind of uncertainties resistible by suitable control methods.

In the case that there are unmatched uncertainties, it is challenging to suppress them because it is hard to formulate these kinds of uncertainties. A common

approach is to apply the available controllers as if there were no unmatched uncertainties. This method will inevitably result in a threshold on the size of the unmatched uncertainties. The unmatched uncertainties are then required to be smaller than the threshold value so that a stability result holds locally with respect to the size of the uncertainties. Since unmatched uncertainties are common in control practice, it is important to suppress them to guarantee the system stability in the presence of significant unmatched uncertainties.

Consequently, the following dynamic model [7] with unmatched uncertainties can be directly formulated by (2.20) without further simplification.

$$\begin{aligned}\dot{x}_1 &= x_2 \\ \dot{x}_2 &= f_1(\mathbf{x}) + b_1(\mathbf{x})u + \zeta_1(\mathbf{x}, u) \\ \dot{x}_3 &= x_4 \\ \dot{x}_4 &= f_2(\mathbf{x}) + b_2(\mathbf{x})u + \zeta_2(\mathbf{x}, u)\end{aligned}\tag{2.20}$$

Here,  $\zeta_1(\mathbf{x}, u) = \Delta f_1(\mathbf{x}) + \Delta b_1(\mathbf{x})u$  and  $\zeta_2(\mathbf{x}, u) = \Delta f_2(\mathbf{x}) + \Delta b_2(\mathbf{x})u$ .

### 2.1.3 Linearized Model

The nonlinear single-pendulum-type overhead crane model has been discussed and it is composed of (2.14) and (2.15). Because  $\theta = 0$  is the sole stable equilibrium of the overhead crane system, both of the equations can be linearized around the point. The linearized equations can be written as

$$(m + M)\ddot{x} + mL\ddot{\theta} = f\tag{2.21}$$

$$\ddot{x} + L\ddot{\theta} + g\theta = 0\tag{2.22}$$

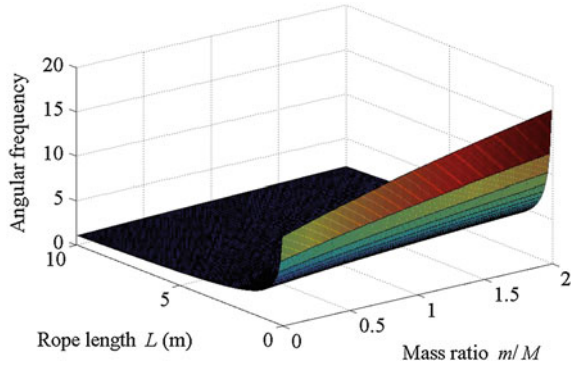
According to Newton's second law,  $f = (m + M)\ddot{x}$  can be obtained. Substituting  $\ddot{x} = f/(m + M)$  into (2.21) yields

$$\frac{f}{M + m} + L\ddot{\theta} + g\theta = 0\tag{2.23}$$

Equation (2.23) is a second order ordinary differential equation. The Laplace transform can be employed to solve Eq. (2.23). Finally, the angular frequency describing the oscillation of the linearized Eq. (2.23) can be formulated as

$$\omega_n = \sqrt{\left(1 + \frac{m}{M}\right)\frac{g}{L}}\tag{2.24}$$

**Fig. 2.2** Variation of the system frequency



Equation (2.24) reveals the system frequency depending on the rope length and the mass ratio. It is of interest to investigate how the frequency changes as a function of the system parameters. Such information can be used for physical insights of the overhead crane system. Figure 2.2 demonstrates the function revealed in (2.24). The MATLAB programs of the example are given in Appendix A.

From Fig. 2.2, the frequency changes very little with respect to the mass ratio when the rope length is more than 4 m. On the other hand, the frequency value has a strong dependence on the mass ratio when the rope length is short.

## 2.1.4 Modeling of Double-Pendulum-Type Cranes

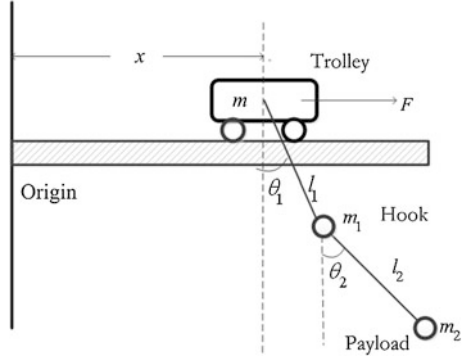
### 2.1.4.1 Modeling

Figure 2.3 illustrates the schematic representation of a double-pendulum-type crane. The crane is moved by a driven force  $F$ , applied to the trolley. This system consists of three subsystems, i.e., trolley, hook, and payload. That is, there exist three variables to describe the crane system. Each subsystem possesses one variable, described by trolley position with respect to the origin,  $x$  (m), hook angle with respect to the vertical line  $\theta_1$  (rad), and payload angle with respect to the vertical line  $\theta_2$  (rad).

Other symbols in Fig. 2.3 are explained as trolley mass  $m_0$  (kg), hook mass  $m_1$  (kg), payload mass  $m_2$  (kg), cable length between trolley and hook  $l_1$  (m), and cable length between hook and payload  $l_2$  (m).

Consider the following ideal assumptions like no friction, massless cables, mass-point hook, and mass-point payload. To obtain the dynamic model of this crane system, the Lagrangian method is also adopted. The following Lagrangian equation with respect to the generalized coordinate  $q_i$  can be obtained as

**Fig. 2.3** Schematic of the double-pendulum-type overhead crane system



$$\frac{d}{dt} \left( \frac{\partial La_d}{\partial \dot{q}_i} \right) - \frac{\partial La_d}{\partial q_i} = T_i \quad (2.25)$$

In (2.25),  $i = 1, 2, 3$ .  $La_d = K_d - P_d$  ( $K_d$  means the system kinetic energy and  $P_d$  denotes the system potential energy.),  $q_i$  is the generalized coordination (here,  $q_1$ ,  $q_2$ , and  $q_3$  indicates  $x$ ,  $\theta_1$ , and  $\theta_2$ , respectively), and  $T_i$  is the external force.

According to the aforementioned assumptions that the payload and hook are regarded as mass-points, the system kinetic energy in Fig. 2.3 can be written as

$$K_d = \frac{1}{2} m_0 \dot{x}^2 + \frac{1}{2} m_1 v_1^2 + \frac{1}{2} m_2 v_2^2 \quad (2.26)$$

here, the vectors  $v_1$  and  $v_2$  denote the hook and payload velocities, respectively. They are defined as

$$\begin{aligned} v_1^2 &= v_{x1}^2 + v_{y1}^2 \\ v_2^2 &= v_{x2}^2 + v_{y2}^2, \end{aligned} \quad (2.27)$$

where  $v_{x1} = \dot{x} + l_1 \dot{\theta}_1 \cos \theta_1$ ,  $v_{y1} = -l_1 \dot{\theta}_1 \sin \theta_1$ ,  $v_{x2} = \dot{x} + l_1 \dot{\theta}_1 \cos \theta_1 + l_2 \dot{\theta}_2 \cos \theta_2$  and  $v_{y2} = -l_1 \dot{\theta}_1 \sin \theta_1 - l_2 \dot{\theta}_2 \sin \theta_2$ .

From Fig. 2.3, the potential energy of the trolley subsystem is kept unchanged. Owing to this fact, the system potential energy in Fig. 2.3 is only exhibited by the potential energies of the hook and payload subsystems, defined as

$$P_d = m_1 g l_1 (1 - \cos \theta_1) + m_2 g [l_1 (1 - \cos \theta_1) + l_2 (1 - \cos \theta_2)] \quad (2.28)$$

Here,  $g$  is the gravitational acceleration. Then,  $La_d$  has the form

$$\begin{aligned}
La_d &= K_d - P_d \\
&= \frac{1}{2}m_0\dot{x}^2 + \frac{1}{2}m_1v_1^2 + \frac{1}{2}m_2v_2^2 \\
&\quad - m_1gl_1(1 - \cos \theta_1) - m_2g[l_1(1 - \cos \theta_1) + l_2(1 - \cos \theta_2)]
\end{aligned} \tag{2.29}$$

Consider the variable  $x$ . Differentiating  $La_d$  with respect to  $x$  in (2.29) yields

$$\frac{\partial La_d}{\partial x} = 0 \tag{2.30}$$

Differentiating  $La_d$  with respect to  $\dot{x}$  in (2.29) yields

$$\frac{\partial La_d}{\partial \dot{x}} = (m_0 + m_1 + m_2)\dot{x} + (m_1 + m_2)l_1\dot{\theta}_1 \cos \theta_1 + m_2l_2\dot{\theta}_2 \cos \theta_2 \tag{2.31}$$

Further, differentiating (2.31) with respect to time  $t$  can have

$$\begin{aligned}
\frac{d}{dt} \left( \frac{\partial La_d}{\partial \dot{x}} \right) - \frac{\partial La_d}{\partial x} &= (m_0 + m_1 + m_2)\ddot{x} + (m_1 + m_2)l_1\ddot{\theta}_1 \cos \theta_1 \\
&\quad - (m_1 + m_2)l_1\dot{\theta}_1^2 \sin \theta_1 + m_2l_2\ddot{\theta}_2 \cos \theta_2 \\
&\quad - m_2l_2\dot{\theta}_2^2 \sin \theta_2
\end{aligned} \tag{2.32}$$

Finally, the Lagrangian equation with respect to  $x$  has the form

$$\begin{aligned}
\frac{d}{dt} \left( \frac{\partial La_d}{\partial \dot{x}} \right) - \frac{\partial La_d}{\partial x} &= (m_0 + m_1 + m_2)\ddot{x} + (m_1 + m_2)l_1\ddot{\theta}_1 \cos \theta_1 \\
&\quad - (m_1 + m_2)l_1\dot{\theta}_1^2 \sin \theta_1 + m_2l_2\ddot{\theta}_2 \cos \theta_2 \\
&\quad - m_2l_2\dot{\theta}_2^2 \sin \theta_2 \\
&= F
\end{aligned} \tag{2.33}$$

Consider the variable  $\theta_1$ . Differentiating  $La_d$  with respect to  $\theta_1$  in (2.29) yields

$$\begin{aligned}
\frac{\partial La_d}{\partial \theta_1} &= -(m_1 + m_2)l_1\dot{x}\dot{\theta}_1 \sin \theta_1 \\
&\quad - m_2l_1l_2\dot{\theta}_1\dot{\theta}_2 \sin(\theta_1 - \theta_2) - (m_1 + m_2)gl_1 \sin \theta_1
\end{aligned} \tag{2.34}$$

Differentiating  $La_d$  with respect to  $\dot{\theta}_1$  in (2.29) yields

$$\frac{\partial La_d}{\partial \dot{\theta}_1} = (m_1 + m_2)(l_1\dot{x} \cos \theta_1 + l_1^2\dot{\theta}_1) + m_2l_1l_2\dot{\theta}_2 \cos(\theta_1 - \theta_2) \tag{2.35}$$

Further, differentiating (2.35) with respect to time  $t$  can have

$$\begin{aligned} \frac{d}{dt} \left( \frac{\partial La_d}{\partial \dot{\theta}_1} \right) &= (m_1 + m_2) \left( l_1 \ddot{x} \cos \theta_1 - l_1 \dot{x} \dot{\theta}_1 \cos \theta_1 + l_1^2 \ddot{\theta}_1 \right) \\ &+ m_2 l_1 l_2 \ddot{\theta}_2 \cos(\theta_1 - \theta_2) - m_2 l_1 l_2 \dot{\theta}_1 \dot{\theta}_2 \sin(\theta_1 - \theta_2) \\ &+ m_2 l_1 l_2 \dot{\theta}_2^2 \sin(\theta_1 - \theta_2) \end{aligned} \quad (2.36)$$

Finally, the Lagrangian equation with respect to  $\theta_1$  has the form

$$\begin{aligned} \frac{d}{dt} \left( \frac{\partial La_d}{\partial \dot{\theta}_1} \right) - \frac{\partial La_d}{\partial \theta_1} &= (m_1 + m_2) l_1 \ddot{x} \cos \theta_1 + (m_1 + m_2) l_1^2 \ddot{\theta}_1 \\ &+ m_2 l_1 l_2 \ddot{\theta}_2 \cos(\theta_1 - \theta_2) + m_2 l_1 l_2 \dot{\theta}_2^2 \sin(\theta_1 - \theta_2) \\ &+ (m_1 + m_2) g l_1 \sin \theta_1 \\ &= 0 \end{aligned} \quad (2.37)$$

Consider the variable  $\theta_2$ . Differentiating  $La_d$  with respect to  $\theta_2$  in (2.29) yields

$$\frac{\partial La_d}{\partial \theta_2} = -m_2 l_1 \dot{x} \dot{\theta}_2 \sin \theta_2 + m_2 l_1 l_2 \dot{\theta}_1 \dot{\theta}_2 \sin(\theta_1 - \theta_2) - m_2 g l_2 \sin \theta_2 \quad (2.38)$$

Differentiating  $La_d$  with respect to  $\dot{\theta}_2$  in (2.29) yields

$$\frac{\partial La_d}{\partial \dot{\theta}_2} = m_2 l_1 \dot{x} \cos \theta_1 + m_2 l_2^2 \dot{\theta}_2 + m_2 l_1 l_2 \dot{\theta}_1 \cos(\theta_1 - \theta_2) \quad (2.39)$$

Further, differentiating (2.39) with respect to time  $t$  can have

$$\begin{aligned} \frac{d}{dt} \left( \frac{\partial La_d}{\partial \dot{\theta}_2} \right) &= m_2 l_2 \ddot{x} \cos \theta_2 - m_2 l_2 \dot{x} \dot{\theta}_2 \cos \theta_2 + m_2 l_2^2 \ddot{\theta}_2 + m_2 l_1 l_2 \ddot{\theta}_1 \cos(\theta_1 - \theta_2) \\ &- m_2 l_1 l_2 \dot{\theta}_1^2 \sin(\theta_1 - \theta_2) + m_2 l_1 l_2 \dot{\theta}_1 \dot{\theta}_2 \sin(\theta_1 - \theta_2) \end{aligned} \quad (2.40)$$

Finally, the Lagrangian equation with respect to  $\theta_2$  has the form

$$\begin{aligned} \frac{d}{dt} \left( \frac{\partial La_d}{\partial \dot{\theta}_2} \right) - \frac{\partial La_d}{\partial \theta_2} &= m_2 l_2 \ddot{x} \cos \theta_2 + m_2 l_2^2 \ddot{\theta}_2 + m_2 l_1 l_2 \ddot{\theta}_1 \cos(\theta_1 - \theta_2) \\ &- m_2 l_1 l_2 \dot{\theta}_1^2 \sin(\theta_1 - \theta_2) + m_2 g l_2 \sin \theta_2 \\ &= 0 \end{aligned} \quad (2.41)$$

From (2.33), (2.37), and (2.41), the dynamic model of the double-pendulum-type overhead crane system with respect to  $x$ ,  $\theta_1$ , and  $\theta_2$  [8] can be obtained by means of the Lagrangian method.

$$(m_0 + m_1 + m_2)\ddot{x} + (m_1 + m_2)l_1\ddot{\theta}_1 \cos \theta_1 + m_2l_2\ddot{\theta}_2 \cos \theta_2 - (m_1 + m_2)l_1\dot{\theta}_1^2 \sin \theta_1 - m_2l_2\dot{\theta}_2^2 \sin \theta_2 = F \quad (2.42)$$

$$(m_1 + m_2)l_1\ddot{x} \cos \theta_1 + (m_1 + m_2)l_1^2\ddot{\theta}_1 + m_2l_1l_2\ddot{\theta}_2 \cos(\theta_1 - \theta_2) + m_2l_1l_2\dot{\theta}_2^2 \sin(\theta_1 - \theta_2) + (m_1 + m_2)gl_1 \sin \theta_1 = 0 \quad (2.43)$$

$$m_2l_2\ddot{x} \cos \theta_2 + m_2l_1l_2\ddot{\theta}_1 \cos(\theta_1 - \theta_2) + m_2l_2^2\ddot{\theta}_2 - m_2l_1l_2\dot{\theta}_1^2 \sin(\theta_1 - \theta_2) + m_2gl_2 \sin \theta_2 = 0 \quad (2.44)$$

Rearrange (2.42), (2.43), and (2.44) in the form of a matrix. The three equations can be rewritten as

$$\mathbf{M}(\mathbf{q})\ddot{\mathbf{q}} + \mathbf{C}(\mathbf{q}, \dot{\mathbf{q}})\dot{\mathbf{q}} + \mathbf{G}(\mathbf{q}) = \boldsymbol{\tau} \quad (2.45)$$

Here,  $\mathbf{q} = [x, \theta_1, \theta_2]^T$  is a vector of the three generalized coordinates,  $\boldsymbol{\tau} = [F, 0, 0]^T$  is a vector of the generalized force,  $g$  is the gravitational acceleration,  $\mathbf{M}(\mathbf{q})$  is a  $3 \times 3$  inertia matrix,  $\mathbf{C}(\mathbf{q}, \dot{\mathbf{q}})\dot{\mathbf{q}}$  is a vector of Coriolis and centripetal torques, and  $\mathbf{G}(\mathbf{q})$  is a vector of the gravitational term.  $\mathbf{M}(\mathbf{q})$ ,  $\mathbf{C}(\mathbf{q}, \dot{\mathbf{q}})$  and  $\mathbf{G}(\mathbf{q})$  are defined as

$$\mathbf{M}(\mathbf{q}) = \begin{bmatrix} m_0 + m_1 + m_2 & (m_1 + m_2)l_1 \cos \theta_1 & m_2l_2 \cos \theta_2 \\ (m_1 + m_2)l_1 \cos \theta_1 & (m_1 + m_2)l_1^2 & m_2l_1l_2 \cos(\theta_1 - \theta_2) \\ m_2l_2 \cos \theta_2 & m_2l_1l_2 \cos(\theta_1 - \theta_2) & m_2l_2^2 \end{bmatrix}$$

$$\mathbf{C}(\mathbf{q}, \dot{\mathbf{q}}) = \begin{bmatrix} 0 & -(m_1 + m_2)l_1\dot{\theta}_1 \sin \theta_1 & -m_2l_2\dot{\theta}_2 \sin \theta_2 \\ 0 & 0 & m_2l_1l_2\dot{\theta}_2 \sin(\theta_1 - \theta_2) \\ 0 & -m_2l_1l_2\dot{\theta}_1 \sin(\theta_1 - \theta_2) & 0 \end{bmatrix}$$

$$\mathbf{G}(\mathbf{q}) = [0 \quad (m_1 + m_2)gl_1 \sin \theta_1 \quad m_2gl_2 \sin \theta_2]^T$$

Further, (2.45) can be transformed to its state space expression. The expression [9, 10] has the form

$$\begin{aligned}
\dot{x}_1 &= x_2 \\
\dot{x}_2 &= f_1(\mathbf{x}) + b_1(\mathbf{x})u \\
\dot{x}_3 &= x_4 \\
\dot{x}_4 &= f_2(\mathbf{x}) + b_2(\mathbf{x})u \\
\dot{x}_5 &= x_6 \\
\dot{x}_6 &= f_3(\mathbf{x}) + b_3(\mathbf{x})u
\end{aligned} \tag{2.46}$$

In (2.46), the vector  $\mathbf{x}$  is defined by  $[x_1, x_2, x_3, x_4, x_5, x_6]^T$ ;  $x_1 = x$ ;  $x_3 = \theta_1$ ;  $x_5 = \theta_2$ ;  $x_2$  is the trolley velocity;  $x_4$  is the angular velocity of the hook;  $x_6$  is the angular velocity of the payload;  $u = F$  is the control input; and  $f_i(\mathbf{x})$  and  $b_i(\mathbf{x})$  ( $i = 1, 2, 3$ ) are nonlinear functions of the vector  $\mathbf{x}$ , formulated by  $f_i(\mathbf{x}) = \Gamma_i/\Delta$  and  $b_i(\mathbf{x}) = T_i/\Delta$ . Here  $\Gamma_i$ ,  $T_i$ , and  $\Delta$  are determined by

$$\begin{aligned}
\Delta &= (m_1 + m_2)m_2l_1^2l_2^2[(m_0 + m_1 + m_2) - (m_1 + m_2)\cos^2(x_3)] \\
&\quad - m_2^2l_1^2l_2^2[(m_1 + m_2)\cos^2(x_5) + (m_0 + m_1 + m_2)\cos^2(x_3 - x_5) \\
&\quad - 2(m_1 + m_2)\cos(x_3)\cos(x_5)\cos(x_3 - x_5)]
\end{aligned}$$

$$\begin{aligned}
\Gamma_1 &= [(m_1 + m_2)m_2l_1^2l_2^2 - m_2^2l_1^2l_2^2\cos^2(x_3 - x_5)][(m_1 + m_2)l_1x_4^2\sin(x_3) \\
&\quad + m_2l_2x_6^2\sin(x_5)] + [(m_1 + m_2)m_2l_1l_2^2\cos(x_3) \\
&\quad - m_2^2l_1l_2^2\cos(x_5)\cos(x_3 - x_5)][m_2l_1l_2x_6^2\sin(x_3 - x_5) \\
&\quad + (m_1 + m_2)gl_1\sin(x_3)] + [(m_1 + m_2)m_2l_1^2l_2\cos(x_5) \\
&\quad - m_2l_1^2l_2\cos(x_3)\cos(x_3 - x_5)][-m_2l_1l_2x_4^2\sin(x_3 - x_5) + m_2gl_2\sin(x_5)]
\end{aligned}$$

$$T_1 = (m_1 + m_2)m_2l_1^2l_2^2 - m_2^2l_1^2l_2^2\cos^2(x_3 - x_5)$$

$$\begin{aligned}
\Gamma_2 &= [m_2^2l_1l_2^2\cos(x_5)\cos(x_3 - x_5) - (m_1 + m_2)m_2l_1l_2^2\cos(x_3)][(m_1 + m_2)l_1x_4^2\sin(x_3) \\
&\quad + m_2l_2x_6^2\sin(x_5)] + [m_2^2l_2^2\cos^2(x_5) - (m_0 + m_1 + m_2)m_2l_2^2][m_2l_1l_2x_6^2\sin(x_3 - x_5) \\
&\quad + (m_1 + m_2)gl_1\sin(x_3)] + [(m_0 + m_1 + m_2)m_2l_1l_2\cos(x_3 - x_5) \\
&\quad - (m_1 + m_2)m_2l_1l_2\cos(x_3)\cos(x_5)][-m_2l_1l_2x_4^2\sin(x_3 - x_5) + m_2gl_2\sin(x_5)]
\end{aligned}$$

$$T_2 = m_2^2l_1^2l_2^2\cos(x_5)\cos(x_3 - x_5) - (m_1 + m_2)m_2l_1l_2^2\cos(x_3)$$

$$\begin{aligned}
\Gamma_3 &= \{(m_1 + m_2)m_2l_1^2l_2[\cos(x_3)\cos(x_3 - x_5) - \cos(x_5)]\}[(m_1 + m_2)l_1x_4^2\sin(x_3) \\
&\quad + m_2l_2x_6^2\sin(x_5)] + [(m_0 + m_1 + m_2)m_2l_1l_2\cos(x_3 - x_5) \\
&\quad - (m_1 + m_2)m_2l_1l_2\cos(x_3)\cos(x_5)][m_2l_1l_2x_6^2\sin(x_3 - x_5) + (m_1 + m_2)gl_1\sin(x_3)] \\
&\quad + [(m_1 + m_2)^2l_1^2\cos^2(x_3) - (m_0 + m_1 + m_2)(m_1 + m_2)l_1^2] \\
&\quad \times [-m_2l_1l_2x_4^2\sin(x_3 - x_5) + m_2gl_2\sin(x_5)]
\end{aligned}$$

$$T_3 = (m_1 + m_2)m_2l_1^2l_2 \cos(x_3) \cos(x_3 - x_5) - (m_1 + m_2)m_2l_1^2l_2 \cos(x_5)$$

Note that the model (2.45) has two important assumptions that are mass-point hook and payload. Usually, the mass-point assumption can be satisfied for the hook subsystem. However, the mass-point assumption for the payload subsystem can be satisfied under some operating conditions. Concerning these extreme operating conditions, the moment of inertia of the payload subsystem cannot be ignored and it has to be taken into consideration.

### 2.1.5 Model with Uncertainties

Equation (2.46) is an ideal model. It can be treated as the nominal model of double-pendulum-type overhead cranes. Considering the system uncertainties, the uncertain equations can be derived from (2.46). The analysis is very similar to the process in Sect. 2.1.2. Briefly, the uncertain model of the double-pendulum-type overhead crane in Fig. 2.1 can be described as

$$\begin{aligned} \dot{x}_1 &= x_2 \\ \dot{x}_2 &= f_1(\mathbf{x}) + b_1(\mathbf{x})u + \xi_1(\mathbf{x}, u) \\ \dot{x}_3 &= x_4 \\ \dot{x}_4 &= f_2(\mathbf{x}) + b_2(\mathbf{x})u + \xi_2(\mathbf{x}, u) \\ \dot{x}_5 &= x_6 \\ \dot{x}_6 &= f_3(\mathbf{x}) + b_3(\mathbf{x})u + \xi_3(\mathbf{x}, u) \end{aligned} \tag{2.47}$$

The uncertain part  $\xi_i(\mathbf{x}, u)$  in (2.47) is matched, if it can be written as  $\xi_i(\mathbf{x}, u) = b_i(\mathbf{x})\Delta\xi_i(\mathbf{x}, u)$  where  $i = 1, 2, 3$ . Otherwise, the three uncertain terms are unmatched because they cannot enter the crane model by the control channel. Note that the three uncertain terms have to be treated as a whole. The uncertainties are still unmatched, if only a part of the three terms can enter the crane model by the control channel.

### 2.1.6 Linearized Model

The nonlinear double-pendulum-type overhead crane model is shown in (2.13). Because  $\theta_1 = \theta_2 = 0$  is the sole stable equilibrium of the double-pendulum-type crane system, (2.13) can be linearized around  $\theta_1 = 0$  and  $\theta_2 = 0$ . The linearized crane model can be written as

$$\bar{M} \ddot{\mathbf{q}} + K \mathbf{q} = 0 \quad (2.48)$$

In the linearized model (2.48), the matrixes  $\bar{M}$  and  $K$  are determined as

$$\bar{M} = \begin{bmatrix} m_0 + m_1 + m_2 & (m_1 + m_2)l_1 & m_2l_2 \\ (m_1 + m_2)l_1 & (m_1 + m_2)l_1^2 & m_2l_1l_2 \\ m_2l_2 & m_2l_1l_2 & m_2l_2^2 \end{bmatrix}$$

$$K = \begin{bmatrix} 0 & 0 & 0 \\ 0 & (m_1 + m_2)gl_1 & 0 \\ 0 & 0 & m_2gl_2 \end{bmatrix}$$

The two natural frequencies of the double-pendulum-type overhead crane system can be obtained by the nonzero eigenvalues of the matrix— $\bar{M} K$ . Their expressions [11] are determined as

$$\omega_1 = \sqrt{\frac{g}{2}(\alpha - \sqrt{\beta})} \quad (2.49)$$

$$\omega_2 = \sqrt{\frac{g}{2}(\alpha + \sqrt{\beta})} \quad (2.50)$$

Here,  $\alpha$  has a form

$$\alpha = \frac{m_1 + m_2}{m_1} \left( \frac{1}{l_1} + \frac{1}{l_2} \right)$$

Another parameter  $\beta$  is formulated as

$$\beta = \left( \frac{m_1 + m_2}{m_1} \right)^2 \left( \frac{1}{l_1} + \frac{1}{l_2} \right)^2 - 4 \left( \frac{m_1 + m_2}{m_1} \right) \frac{1}{l_1l_2}$$

From (2.49) and (2.50), the two natural frequencies not only depend on the length of the cables but also depend on the masses of payload and hook. It is interesting to investigate how the frequencies change as a function of the system physical parameters.

To simplify this problem,  $R = m_2/m_1$  is defined as the payload-to-hook mass ratio, the cable length between hook and payload  $l_2$  is considered as a variable when the total length  $l$  determined by  $l_1$  plus  $l_2$  is held constant at 6 m. Figure 2.4 illustrates the two oscillation frequencies as a function of  $R$  and  $l_2$ .

In Fig. 2.4,  $\omega_1$  changes very little for a constant  $l_1 + l_2$ . It corresponds closely to the frequency of a single pendulum with the length of  $l_1 + l_2$ . On the other hand, the value of  $\omega_1$  is maximized for a constant  $l_1 + l_2$  when the two cable lengths are equal to  $\frac{l_1+l_2}{2}$ , but it can be dramatically changed by the hoisting operation [12].

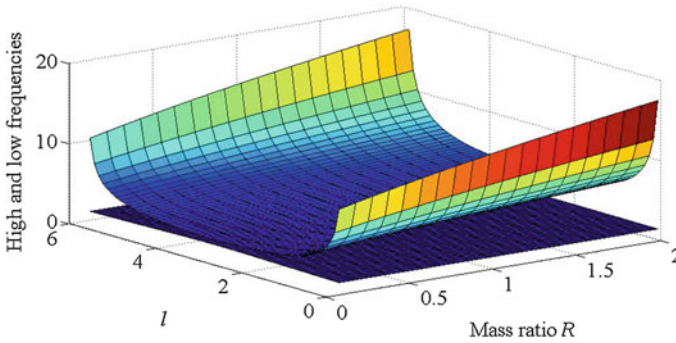


**Fig. 2.4** Variation of the two frequencies

Furthermore, the high-frequency  $\omega_2$  has a strong dependence on the cable length  $l_2$ ; the value of  $\omega_2$  varies substantially more than the value of  $\omega_1$ , the contribution of  $\omega_2$  to problematic swing amplitude is particularly large for a constant  $l_1 + l_2$  when the two cable lengths are approximately equal.

Concerning the mass ratio,  $R$  has a relatively small effect on  $\omega_1$ , but the high-frequency  $\omega_2$  becomes more important to the double-pendulum motions for low payload-to-hook mass ratios. In brief, low payload-to-hook mass ratios and equal cable lengths are more representative to depict the double-pendulum motions of the crane for the point-to-point transport control with a constant  $l_1 + l_2$ .

## Appendices

### *A Matlab Codes to Plot Fig. 2.2*

```
k=0.01:0.01:2; % Mass ratio from 0.01 to 2, every each 0.01.
l=0.1:0.1:10; % Rope length from 0.1 to 10, every each 0.1
[K,L]=meshgrid(k,l); % K and L arrays for 3-D plots.
w=sqrt((1+K)*9.8./L); % Array of angular frequency
surf(K,L,w) % 3-D colored surface.
```

## ***B Matlab Codes to Plot Fig. 2.4***

```

r=0.1:0.1:2;           %mass ratio
l2=0.1:0.1:6;         %cable length between hook and payload
l1=6-l2;              %l1 plus l2 is held constant at 6m
g=9.8;                % gravitational acceleration
[R,L2]=meshgrid(r,l2); % R and L2 arrays for 3-D plots
p=sqrt((1+R).^2.*(1./(6-L2)+1./L2).^2-4.*((1+R)./(L2.*(6-L2))));
w1=sqrt(g/2).*sqrt((1+R).*(1./(6-L2)+1./L2)-p); % Array of w1
w2=sqrt(g/2).*sqrt((1+R).*(1./(6-L2)+1./L2)+p); % Array of w2
surf(R,L2,w1)         %3-D colored surface
hold;                 % Another surface
surf(R,L2,w2)         %3-D colored surface

```

## **References**

1. Abdel-Rahman EM, Nayfeh AH, Masoud ZN (2003) Dynamics and control of cranes: a review. *J Vib Control* 9(7):863–908
2. Lee HH (1998) Modeling and control of a three-dimensional overhead crane. *J Dyn Syst Meas Control Trans ASME* 120(4):471–476
3. Spong MW, Hutchinson S, Vidyasagar M (2006) *Robot modeling and control*. Wiley, New York
4. Oguamanam D, Hansen JS, Heppler G (2001) Dynamics of a three-dimensional overhead crane system. *J Sound Vib* 242(3):411–426
5. Liu D, Yi J, Zhao D, Wang W (2005) Adaptive sliding mode fuzzy control for a two-dimensional overhead crane. *Mechatronics* 15(5):505–522
6. Cheng C, Chen CY (1996) Controller design for an overhead crane system with uncreinty. *Control Eng Pract* 4(5):645–653
7. Park MS, Chwa D, Hong SK (2008) Antisway tracking control of overhead cranes with system uncertainty and actuator nonlinearity using an adaptive fuzzy sliding-mode control. *IEEE Trans Ind Electron* 55(11):3972–3984
8. Tuan LA, Lee SG (2013) Sliding mode controls of double-pendulum crane systems. *J Mech Sci Technol* 27(6):1863–1873
9. Liu D, Guo W, Yi J (2008) Dynamics and GA-based stable control for a class of underactuated mechanical systems. *Int J Control Autom Syst* 6(1):35–43
10. O'Connor W, Habibi H (2013) Gantry crane control of a double-pendulum, distributed-mass load using mechanical wave concepts. *Mech Sci* 4:251–261
11. Vaughan J, Kim D, Singhose W (2010) Control of tower cranes with double-pendulum payload dynamics. *IEEE Trans Control Syst Technol* 18(6):1345–1358
12. Singhose W, Kim D, Kenison M (2008) Input shaping control of double-pendulum bridge crane oscillations. *J Dyn Syst Meas Control Trans ASME* 130(3): doi:[10.1115/1.2907363](https://doi.org/10.1115/1.2907363)



<http://www.springer.com/978-3-662-48415-9>

Hierarchical Sliding Mode Control for Under-actuated  
Cranes

Design, Analysis and Simulation

Qian, D.; Yi, J.

2015, XIV, 199 p. 93 illus., 38 illus. in color., Hardcover

ISBN: 978-3-662-48415-9